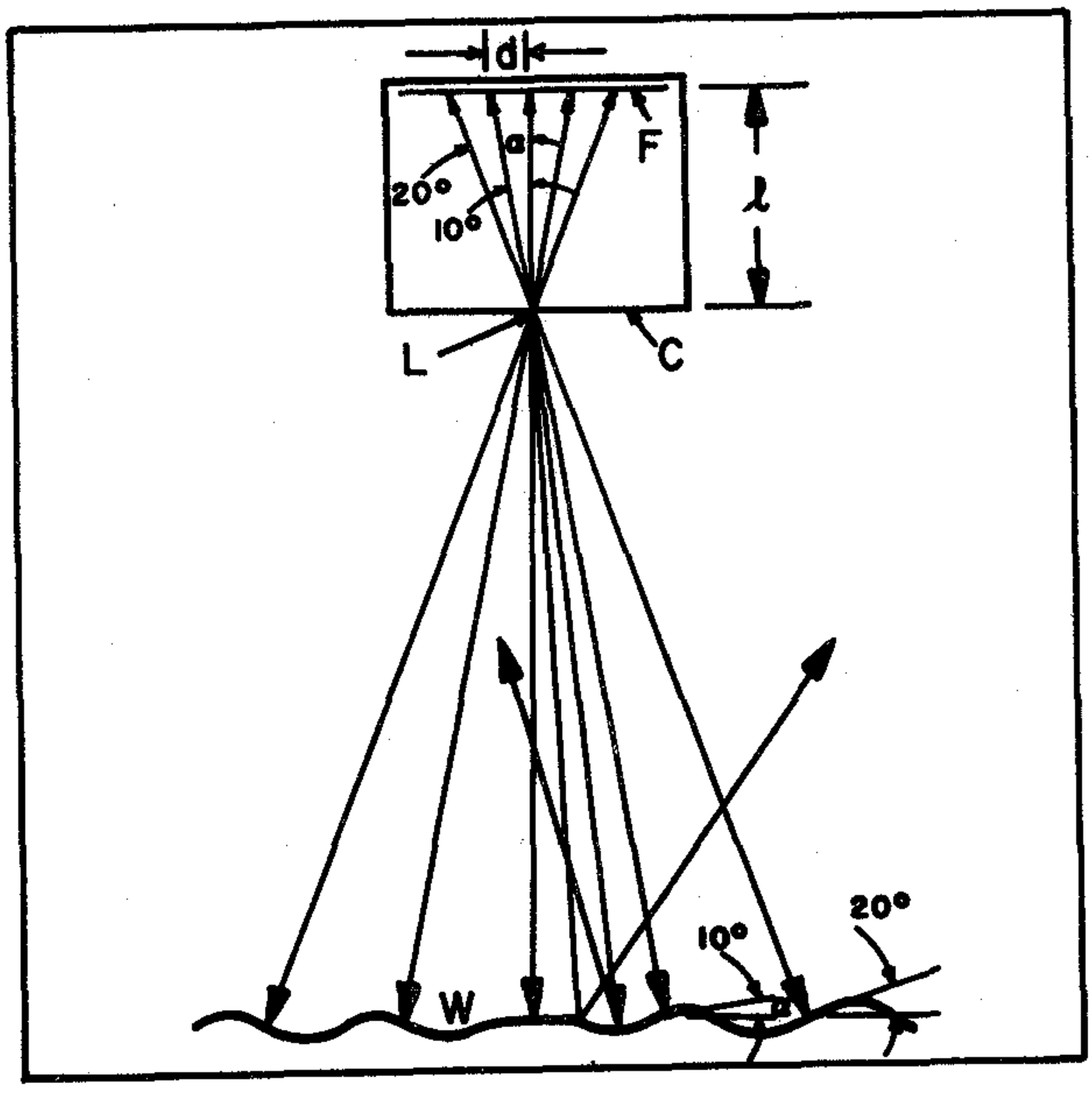

FIG. 12.32 Camera geometry for Schooley's flash photography measurements of wave slopes.

support for his experiment. The resulting photographs reveal flash reflection patterns that can readily be converted into water wave slope data. The associated geometry is vastly simpler than in the case of Cox and Munk. However, the presence of the bridge and river shoreline, as in the similar case of the presence of Duntley's sea state meter supports and nearby shoreline, contribute a measure of unwanted hydrodynamic effects. Nevertheless, the simple geometry of the experiment, depicted schematically in Fig. 12.32, leads with a minimum of analytical effort to results not too greatly different from the general type of results of Cox and Munk, and Duntley. Thus, for example, the standard deviation of the crosswind wave slopes was found to be approximately 2.5, 5, and 7.8 *degrees* for surface wind speeds of 5, 10, and 20 knots, respectively. Under the same conditions the up-down wind standard deviations were found to be 4.2, 7.5, and 10 degrees. The differences between Schooley's results and Cox and Munk's results is that Schooley's results, wind speed for wind speed, are seen to yield too low mean square slopes. This perhaps could be attributed, as suggested by Cox and Munk, to the short wind fetch distances on the river not permitting sufficient build up of wave slopes; and also imperfect resolution of the highlighted areas on Schooley's photographs. (For an indirect route to the wave-slope wind-speed law from a rather unexpected direction, see (12) of Sec. 12.8.)

12.6 Wave Generation and Decay Data

In this section we shall review those phases of the growth and decay of wind-generated waves pertinent to our

present optical studies of the air-water surface. Most of the properties presented below are relatively precise quantitative empirical facts about our ordinary intuitive understanding of wave phenomena. These data have been gathered over the years by various workers and are beginning to form a coherent picture of the generation and decay of wind-generated waves on the air-water surface. For workers in the field of hydrologic optics, some knowledge of the basic facts of the generation and decay of water waves will be helpful in predicting the optical state of the sea in a region, having given the wind histories, fetch lengths, and some data on initial wave heights and wave speeds.

Generation of Waves: Shallow Depths, Small Fetches

The generation of waves is replete with intricate effects. We shall describe these features on two levels of detail: first for shallow depth and small fetches, which will allow detailed phenomena to be observed. Then the wave generation over oceanic depths and distances will be discussed.

When the air above a still air-water surface is slowly set into smooth horizontal motion, there is no perceptible disturbance in the smooth surface. If this smoothness (laminar type) of flow is maintained as the air speed increases somewhat, the surface remains unperturbed. However, if the surface has any sort of nonplanar irregularity, produced perhaps by the dropping of a bit of foreign matter on the surface, or if the flow of the air is but the slightest *non*laminar, then the irregularity may grow, under the prodding of the air flow into a wave of increasing length and height. Our studies of the Kelvin-Helmholtz instability ((89) of Sec. 12.3) showed that an air speed of 6.6 m/sec is sufficient to cause such irregularities to develop into growing wavelike disturbances in the surface. Actually, in nature purely laminar air flows are rare: every breeze, no matter how small its speed over the water surface, has small irregular vertical components which cause pressure dimples in the water. The passing air can swirl into and push these dimples, thereby yielding up some of its energy to the water and which, in turn, promptly cashes it in for additional wave amplitude and wavelength. And so waves begin to grow.

In 1951 Roll [266] made some detailed observations on the growth of waves in the ponds of the tidal flats at Neuwerk off the Frisian coast in the Netherlands. Wave growths were observed over fetches of 70 m starting on the windward side of the ponds. Despite the shallowness of the ponds, the depth of the water usually exceeded half a wavelength, and the smallness of the ponds still permitted steady state conditions to be attained shortly after changes of wind direction. In Fig. 12.33 (adapted from [307]) a set of curves are given, each curve being associated with a given fetch. The curves show the wavelength of the wind-generated waves as a function of wind speed U_a. These graphs under careful study tell a remarkable story. For example, if the wind were blowing at 200 cm/sec, small transitional capillary waves of 1.7 cm wavelength would be formed first. This wavelength, as we

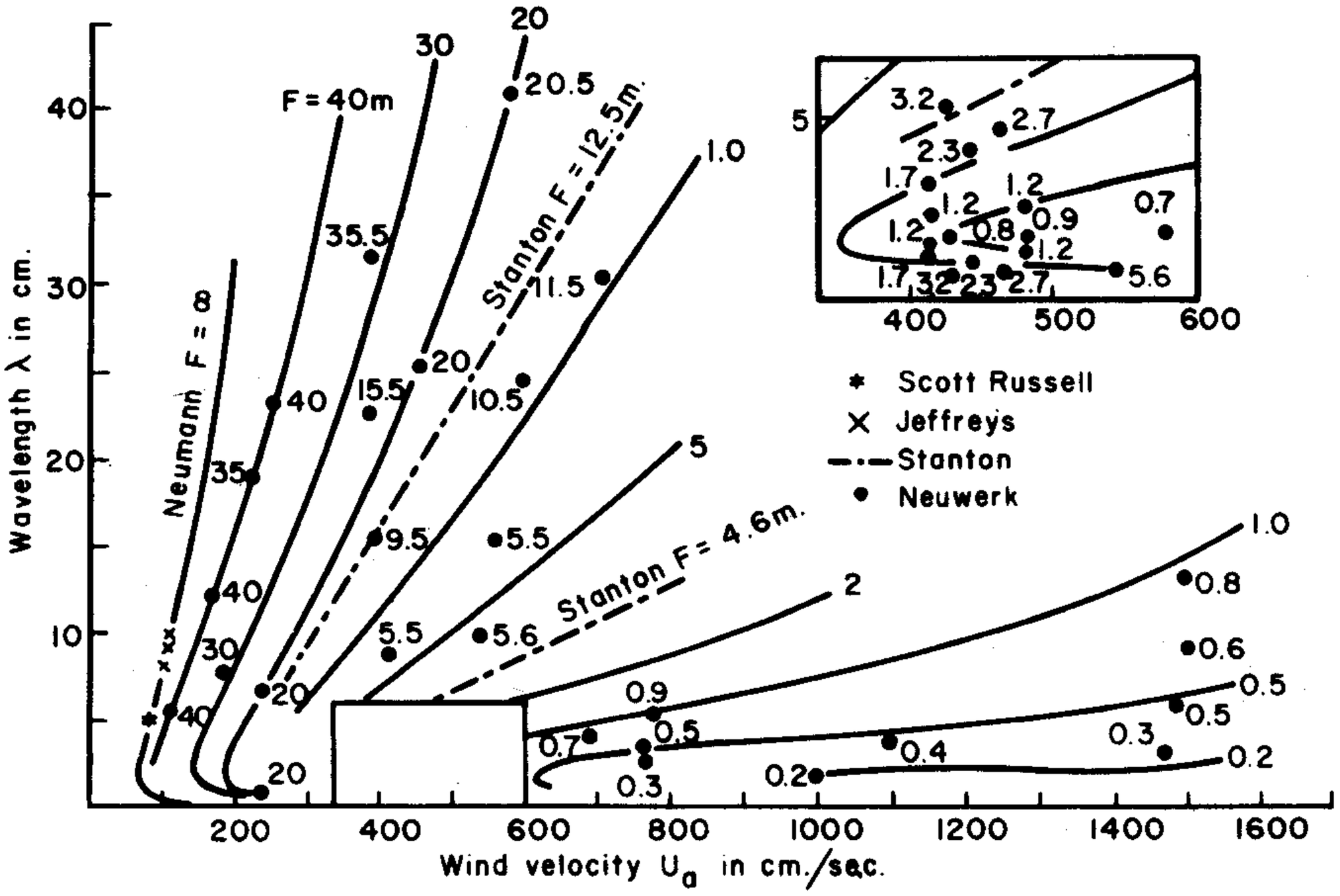

FIG. 12.33 Wavelength λ of wind generated waves as a function of air speed U_a (at 35 cm above the surface) and fetch F, from data by Roll taken in 1951.

have seen ((93) of Sec. 12.3), lies on the borderland between capillary (or surface tension waves) and the larger gravity waves. The graphs show that as the waves progress and the fetch increases, these transitional waves suddenly split apart at about 20 m fetch, aided no doubt by the nonlaminar flow of the air. As the fetch increases farther, say to 30 m, there are now two sets of waves, one of wavelength about 1 cm, the other of wavelength about 7 cm. Generally speaking, as the fetch increases still farther, the big waves get bigger and the smaller waves get smaller. The steepness of the waves at the time of splitting may approach the ratio 1 to 7 (height to length) but generally the gravity waves' slopes diminish with fetch. The graphs also show that the greater the wind speed, the smaller the fetch at which the split takes place. This splitting is signalled in the graph by a vertical tangent to the particular fetch curve.

In exact radiative transfer calculations both wave height and wave slope data are important. Thus the laboratory experiment of Cox [54] documenting the growth with fetch of the mean square wave slope serves to complement the findings of Roll on wavelengths and wave heights. Figure 12.35 depicts mean square slope as a function of wind speed for three different fetches in a laboratory water tunnel shown in Fig. 12.34. Figure 12.36 gives some information on the growth of mean square slopes with fetch for five different wind speeds.

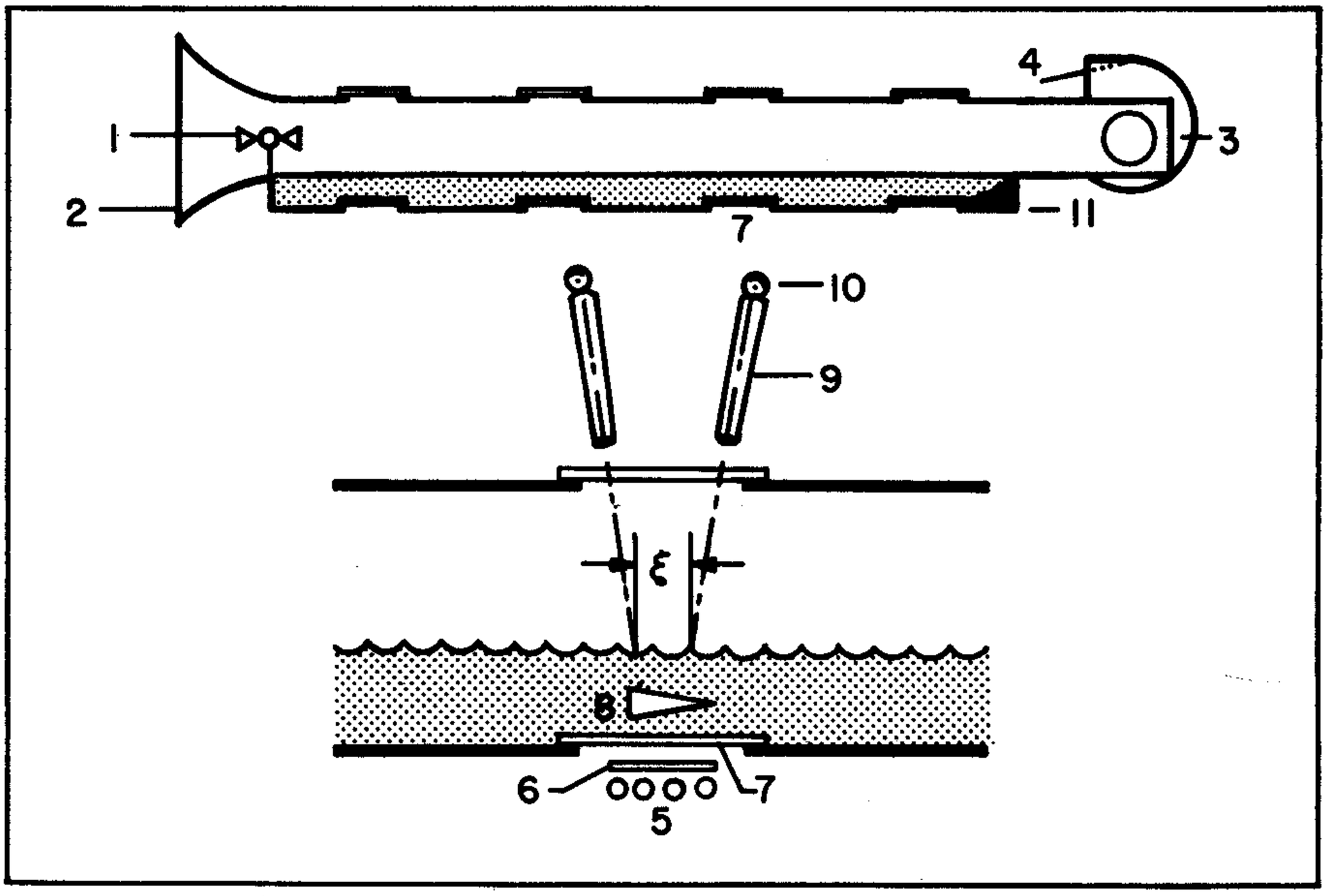

FIG. 12.34 The laboratory wind and water tunnel, as devised by Cox, for measurements of wind generated wave slopes. A cup anemometer (1) measures the wind speed in the entrance nozzle (2) as the wind sweeps over the water (dotted) and is drawn through the tunnel by a fan (3). The wind speed is controlled by a damper (4). Observations of the waves are possible through a set of viewing ports all along the ceiling of the tunnel. The inset shows the detail of a viewing port. Light sources (5) send light through a diffusing plate (6) and on through a plate-glass window (7) and past a neutral filter wedge (8). A telescope tube (9) focusses an image of the water surface on a pinhole in front of a photocell (10) which leads to a recorder (not shown). Counterflowing waves generated at the end of the tunnel were dampened by a gravel beach (11). The dimensions of the tunnel are 14 cm (depth), 26.3 cm (breadth), 6.1 m (length).

The phenomenon of a minimum-speed wave, of 1.7 cm wavelength, splitting into a distinct pair of capillary and gravity waves as observed by Roll, was also observed by Schooley [276]. However, the more interesting contribution by Schooley in [276] was the experimental verification of the detailed geometric structure of the wind-generated capillary waves. Recall from our hydrodynamic studies in Sec. 12.3 that the linearized theory was able to predict precisely the celerity-wavelength relationship for capillary waves ((95) of Sec. 12.3). However, the true shape of the capillary waves of *finite amplitude* was beyond the ken of the linearized theory. The exact shape of capillary waves (as in the case of gravity waves) of finite amplitude, such as those seen being generated by the wind, is a difficult problem in nonlinear differential equation theory which has only recently been solved by Crapper

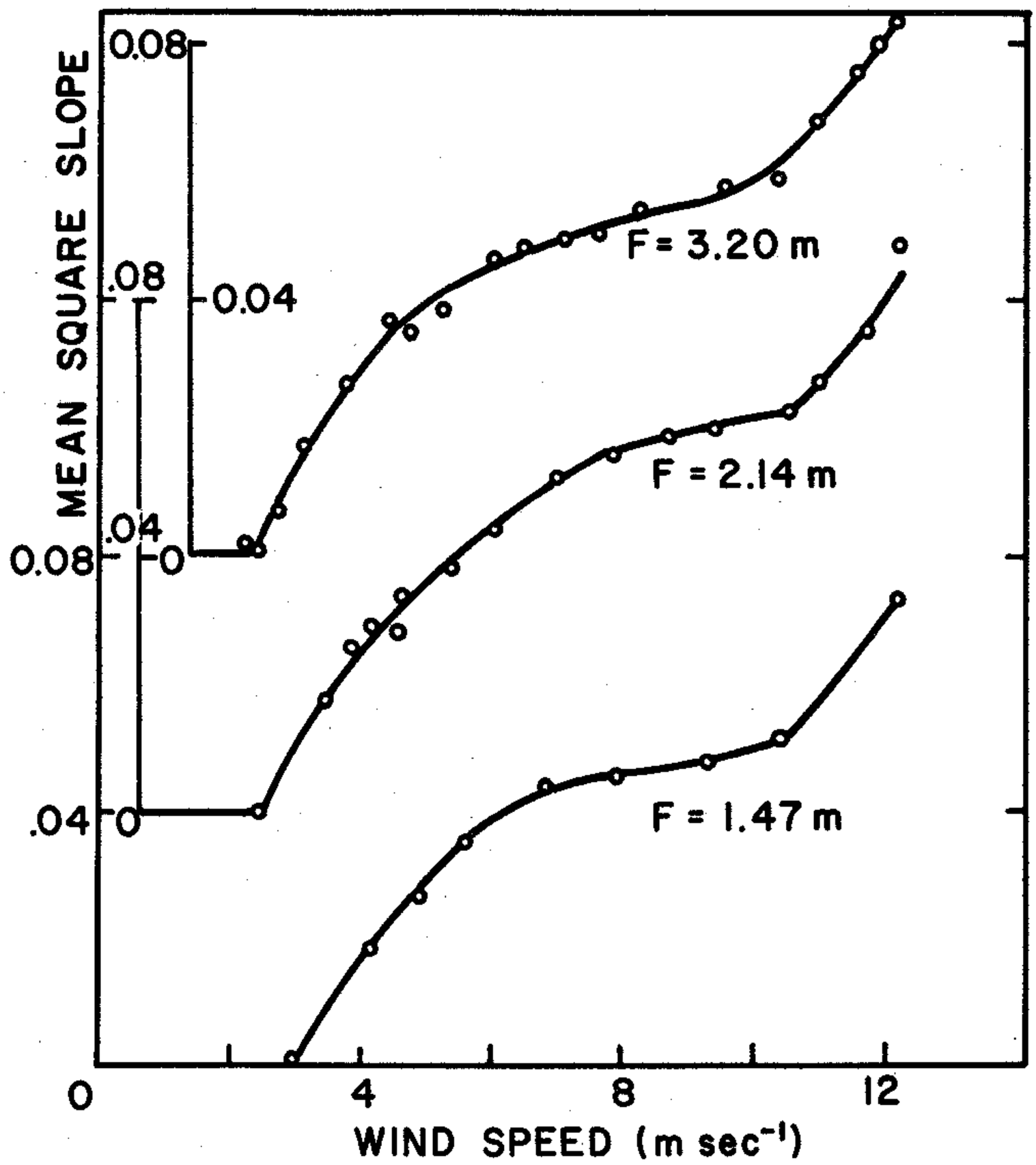

FIG. 12.35 Upwind mean square slope σ_u^2 as measured in the wind tunnel of Fig. 12.34, for the indicated fetches F.

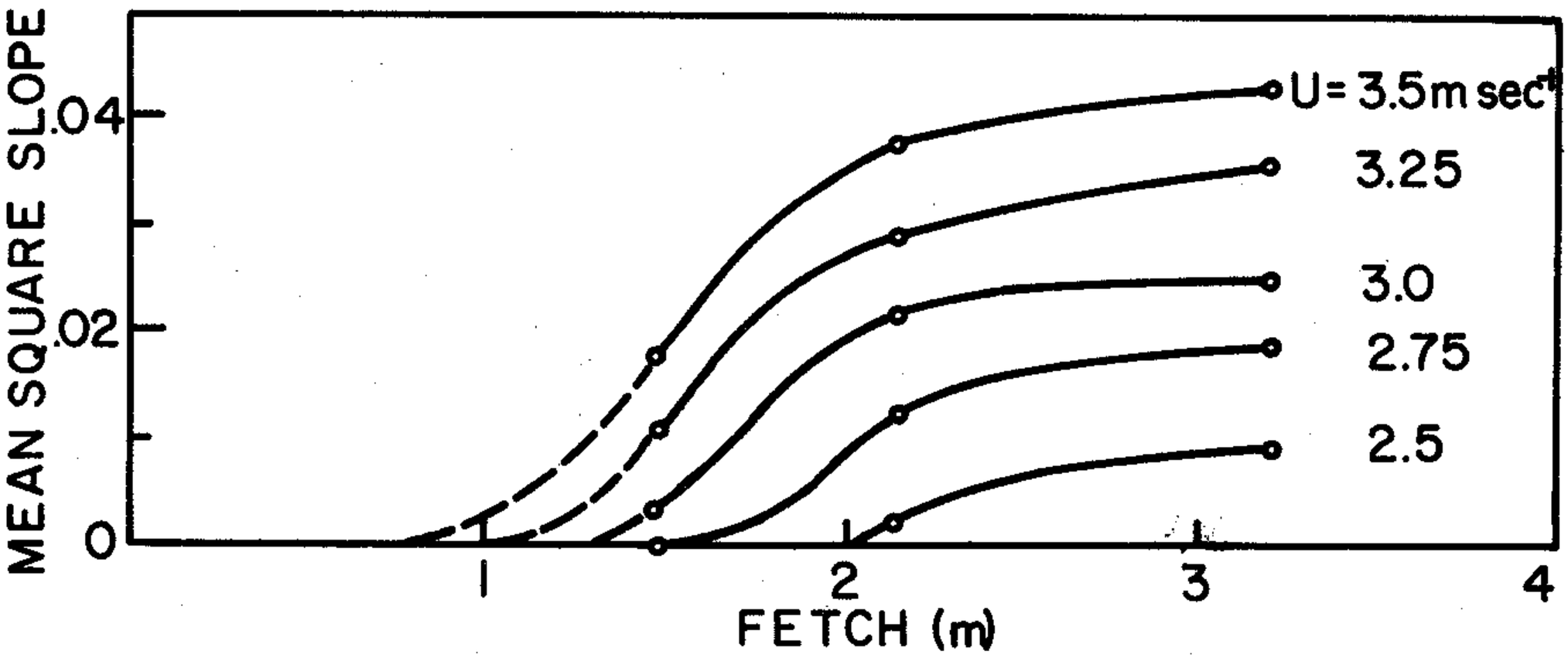

FIG. 12.36 Upwind mean square slope σ_u^2 as a function of fetch for various windspeeds as derived from the graphs of Fig. 12.35

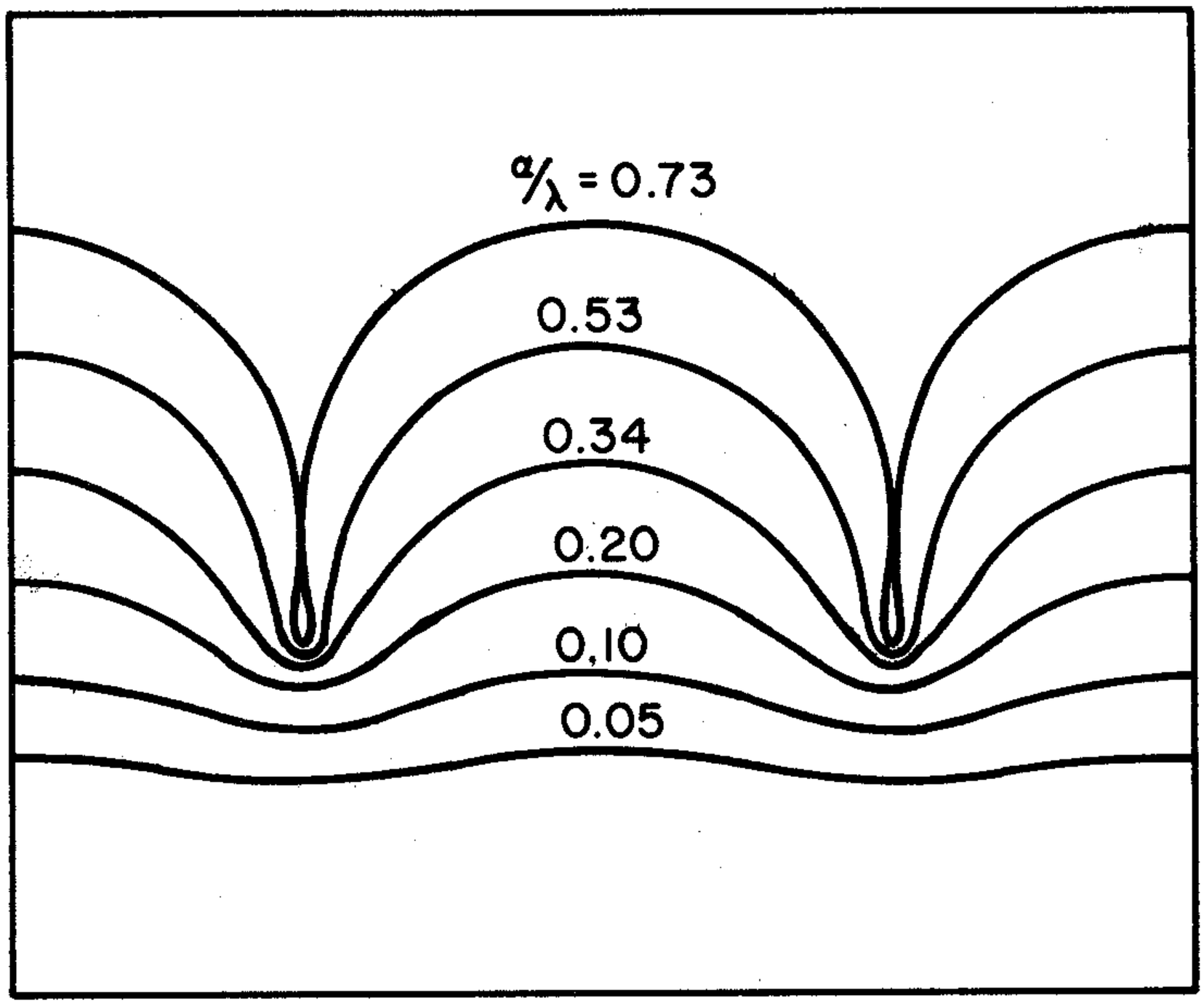

FIG. 12.37 Theoretical capillary wave profiles for various amplitude/wavelength ratios (a/λ), as predicted via Crapper's analysis.

[60]. Schooley verified the theory by reproducing capillary wave shapes of the predicted kind. A sample of shapes is shown in Fig. 12.37. According to the linearized hydrodynamic theory, solitary gravity waves customarily occur in sinusoidal form with very small (infinitesimal) heights in the air-water surface and have relatively gently sloped configurations. For gravity waves of finite height, the configurations are approximately trochoidal with configurations not exceeding 1 to 7, depth to length; and if they have vertical crest-cusps--these will occur with tangents not exceeding 30° from the horizontal (cf. Arts. 250-252, [149]). The shape of finite capillary waves, on the other hand, seem turned inside out relative to the trochoidal gravity wave shapes; that is, in capillaries the cusp is a wedge of air pointing down into the water; whereas in finite gravity waves, the cusp is a wedge of water pointing up into the air.

Generation of Waves: Deep Depths, Large Fetches

Extensive observations over the years of the relations between wind speed, wind duration, fetch, wave height, and wave speed of oceanic waves and waves of other extensive natural hydrosols, have resulted in a comprehensive, orderly picture of the empirical and theoretical interconnections among arbitrary pairs of these parameters. One of the first systematic modern compilations was made by Sverdrup and Munk [293], which was later extended by Bretschneider [32] with

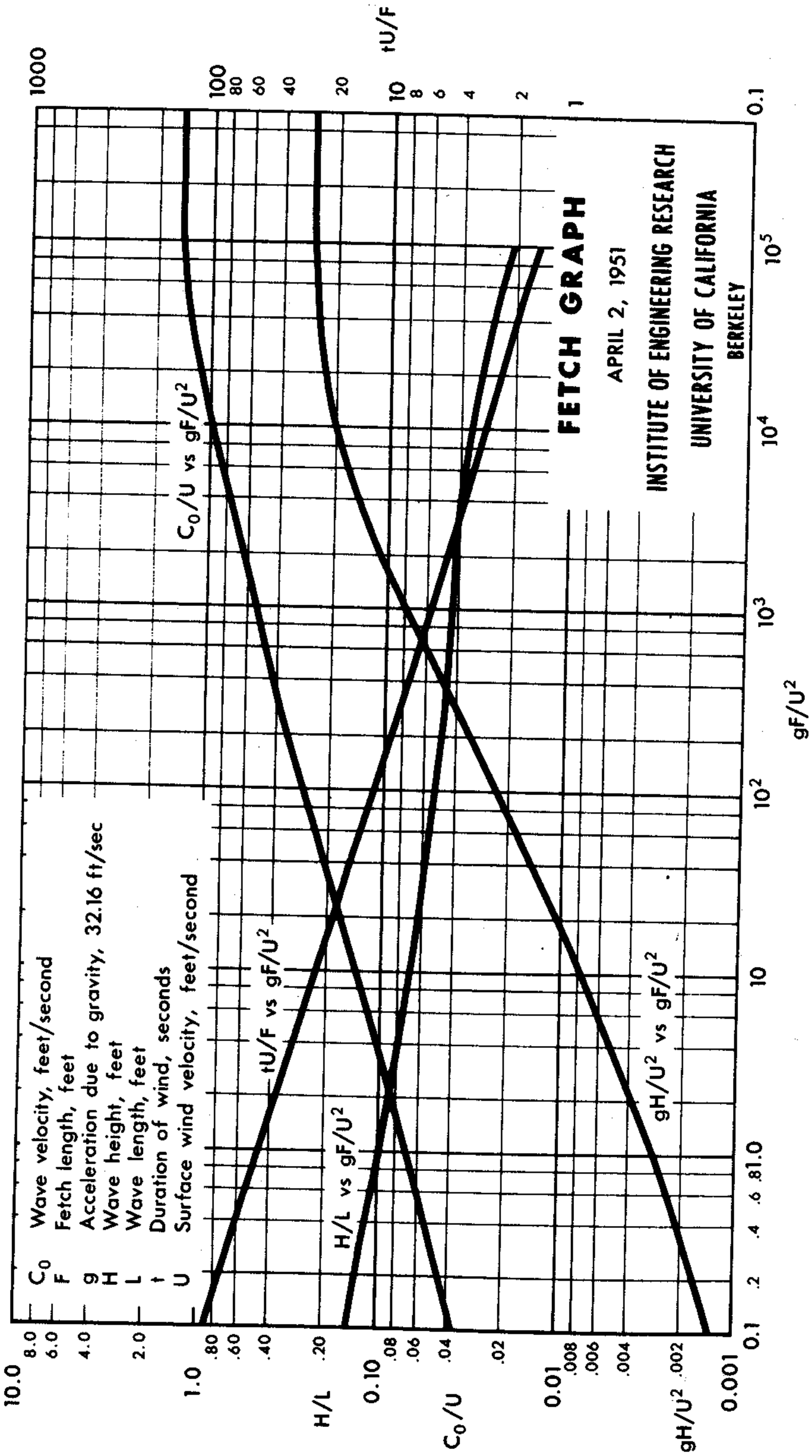

FIG. 12.38 Fetch graph as compiled by Bretschneider from empirical observations of many independent research studies (see text for references and example of use).

additional data. Appropriate references for these data are given in [32]. These data are redrawn and briefly summarized in Fig. 12.38. For a related laboratory study, see [129]. A useful related reference on wave generation, decay, spectra, and statistics is [205].

In using Fig. 12.38, it is important to note that, in the present discussion and that on wave decay below, "wave height " means "significant wave height," a concept evolved by oceanographers in an attempt to attain a usable measure of the height of sea waves when all are visually different one from the other and no mathematically clearcut definition of "wave" or "wave height" is available. The concept of significant wave height may be defined as follows: record all the wave heights going by a fixed point during a test period T_p (recall that a wave height is the vertical distance from crest to trough and is twice the amplitude) and rearrange the recorded heights in order of decreasing height. Say the heights are $H_1, H_2, \ldots, H_N$ so that $H_1 \geq H_2 \geq \ldots \geq H_N$. Divide the group into three equal parts (suppose for this purpose, $N = 3M$); take the first part $H_1, H_2, \ldots, H_M$, and find the average: $\overline{H}_{1/3} = (1/M)(H_1 + H_2 + \ldots + H_M)$. (A practical method of determining M, and also a clarification of what is meant by "wave" is given below.)

Errata

The resultant average is the *significant wave height* for the wave record taken during the test period T_p. When seas are steady, that is in equilibrium, the significant wave height is usually independent of T_p for large T_p. Hence, in a word, the significant wave height of a sample is the average of the heights of the *highest one-third of the waves* in that sample. The significant wave heights in Fig. 12.38 are steady state (i.e., equilibrium) heights, in the sense explained in the example below.

A significant wave period can be associated with the significant wave height as follows. As is well known, waves often travel in closely packed visually observable groups which are the superimposed results of aggregates of component waves. The average period T of these groups (each thought of as a single "wave") observed over a test period T_p is called the *significant wave period.* If we form the quotient T_p/T, we obtain and estimate of the number of such wave groups observed during T_p. Then $(1/3)(T_p/T)$ is the number M (to the nearest integer) of waves used in the computation of the significant wave height above. The significant wave period T and associated wavelength L are related by: $T = \sqrt{2\pi L/g}$, in the notation of Fig. 12.38. The significant wave period used in the Fetch graph is the steady state period.

In seas whose wave spectra are fairly narrow, in the sense that wave heights are confined to a narrow wave height or frequency range, it may be shown [164] that:

$$\text{(significant wave height)} = 1.600 \text{ (average wave height)}$$

$$(\overline{H}_{1/3}) = 1.600\ (\overline{H}_1) \qquad (1)$$

and that:

(significant wave height) = 1.416 (root mean square height)

(2)

i.e.,

$$(\overline{H}_{1/3}) = 1.416(\overline{H}) \quad .$$

In the paper [164], a comparison with experimental data was made which shows that the relationships (1) and (2) are quite accurate. In this way we can use Fig. 12.38 and (2) to estimate the mean square elevation $\overline{\zeta^2}$, used in the theory of Sec. 12.11, under various hydrologic conditions. The connection between the mean square elevation $\overline{\zeta^2}$ and the mean square height $\overline{H}^2$ is:

$$(\overline{H})^2 = 4\overline{\zeta^2} \quad . \tag{3}$$

We shall use "$\overline{H}_{1/3}$" when it is necessary to be quite specific about significant wave height; otherwise, for brevity, the bar and "1/3" will be dropped from "$\overline{H}_{1/3}$".

As an example of the use of Fig. 12.38, suppose we required the root mean square elevation of the wind generated waves in an oceanic region for which the following wind and fetch information is known: The waves in the region were generated by 20 mile per hour surface winds over a fetch F of about 20 miles during a five hour period, t. These estimates are of course order-of-magnitude estimates at best in present-day meteorologic technology and will be treated accordingly. Hence, converting to the units used by the Fetch Graph, $F = 20 \times (5 \times 10^3) = 10^5$ feet. $t = 5 \times 3600 = 1.8 \times 10^4$ sec. $U = 20 \times 1.47 = 29.4$ feet/sec. We shall use the graph of gH/U^2, since we know F, and U, and of course $g = 32.16$ feet/sec^2. But what role does t play? It is known from extensive observations and theoretical analysis that for a given fetch length and wind speed, there is a time t beyond which the generated waves reach an equilibrium steady state in height and period. This limiting time is the time it would take the energy front associated with the significant waves to propagate, at the continuously changing group velocity, from the beginning to the end of the fetch [32]. This empirical connection between t, U and F is included in Fig. 12.38. To see if the given time of 5 hours is a steady state time, we compute gF/U^2

$$gF/U^2 = \frac{32.16 \times 10^5}{(29.4)^2} = 3.72 \times 10^3 \quad .$$

With this value as abscissa, we find the corresponding ordinate on the tU/F vs. gF/U^2 curve to be

$$tU/F = 4$$

so that

$$t = 4F/U = 1.36 \times 10^4 \text{ seconds}$$

which is the time for the wind-generated waves to reach a steady state over the given fetch and under the given wind speed. Since our given generating time is 1.8×10^4 sec, it appears that we may use the gH/U^2 vs. gF/U^2 curve to estimate H. We have already reckoned gF/U^2; we find that the corresponding ordinate is:

$$gH/U^2 = 0.15$$

so that

$$H = 0.15 \times \frac{U^2}{g} = 4.03 \text{ feet}$$

which is the steady state significant wave height at the end of the 20-mile fetch generated by the 20 mile per hour winds. By (3) the associated root mean square elevation is

$$\sqrt{\overline{\zeta^2}} = \frac{4.03}{2.83} = 1.42 \text{ feet.}$$

If it turns out that a given wave generating wind has a duration less then the steady state wind, then clearly Fig. 12.38 can only give an upper bound to $\overline{\zeta^2}$.

Decay of Waves

When the wave-generating ocean winds decrease or die away, their wave progeny may continue for thousands of miles, dissipating and decreasing in their energies and heights continuously as they travel along into relatively still water. Initially, the greater waves leave behind their smaller companions by sheer speed ((68) of Sec. 12.3), the net result being a spreading out in space of the original collection of waves. (This is analogous to the dispersion of light waves in material media.) Empirical studies have shown that the height and period of decaying water wave groups, at any stage in their decay-run, depend principally on three factors: the length of the fetch over which they were generated, and the height and period with which they began their decay-run.

In order to describe the observed dependences on these parameters, we shall write:

"T_F" for significant wave period at end of fetch F

"H_F" for significant wave height at end of fetch F

"T_D" for significant wave period at end of decay distance D

"H_D" for significant wave height at end of decay distance D.

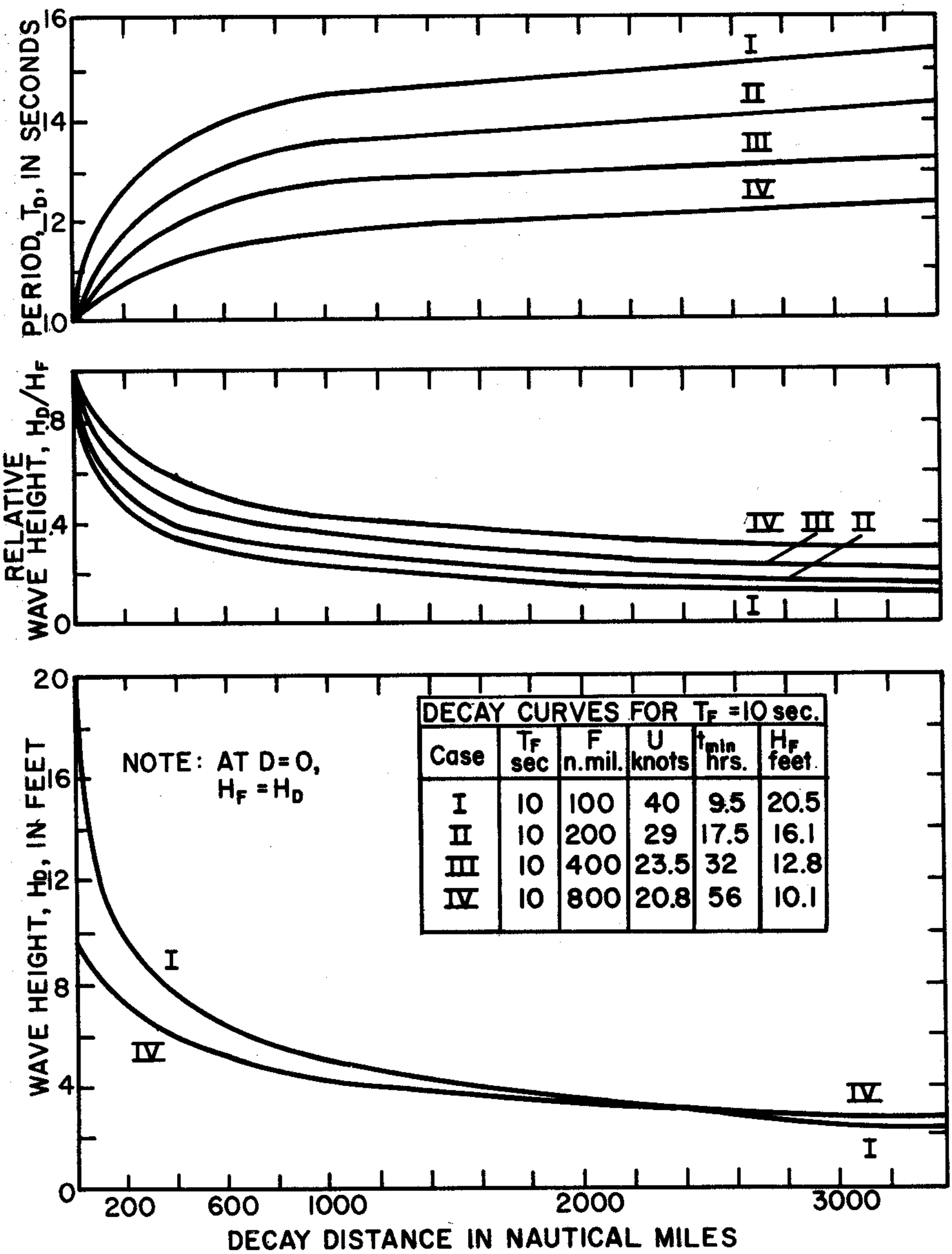

FIG. 12.39(a) An example of how wave heights decrease and wave periods increase with decay distance. This set of graphs for T_f = 10 sec and the indicated cases (after Bretschneider).

Figure 12.39(a) and Fig. 12.39(b), adapted from [32], gives an example of these four quantities as a function of the decay distance D. All graphs in (a) refer to a T_F of 10 sec. Observe

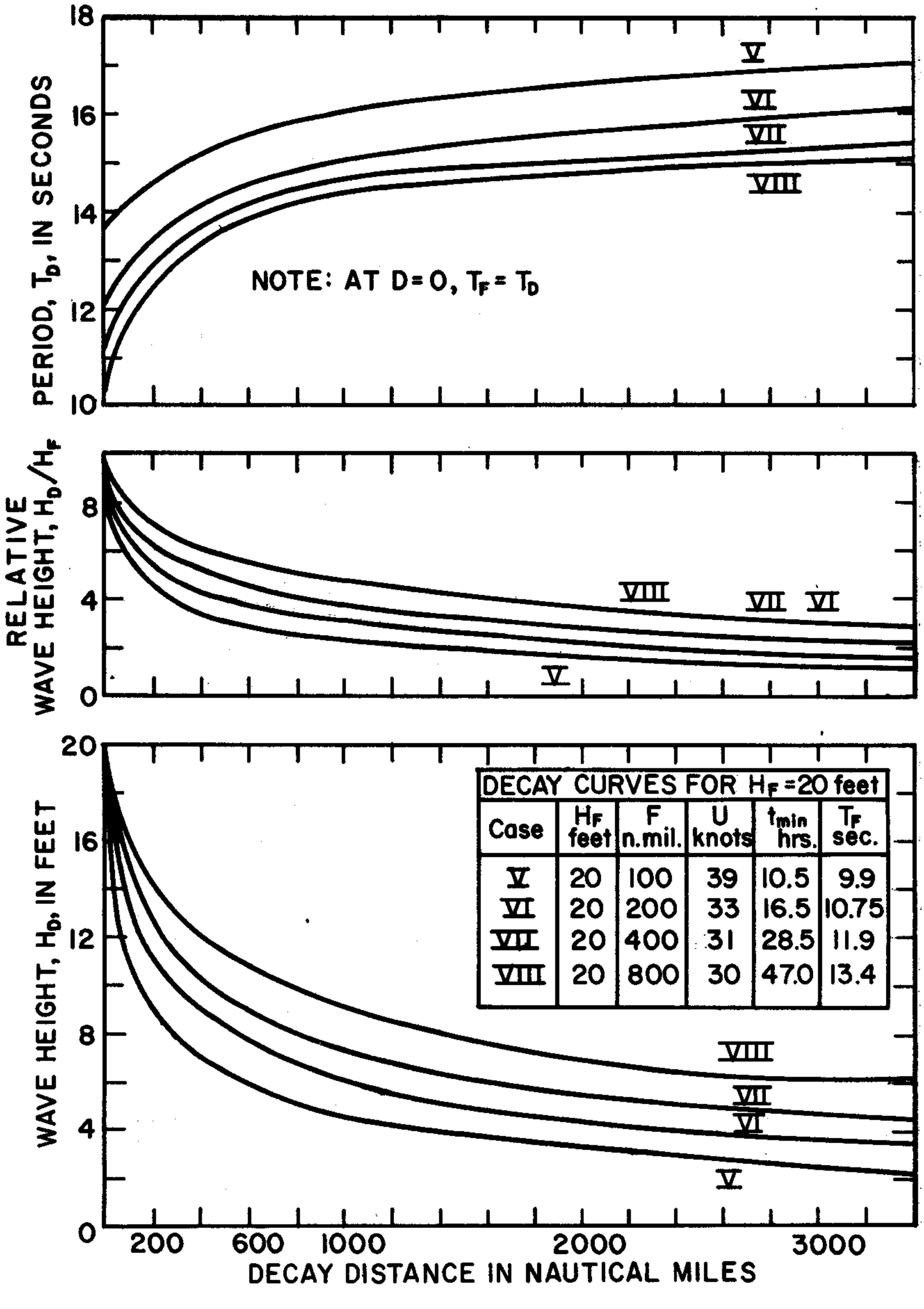

FIG. 12.39(b) An example of how wave heights decrease and wave periods increase with decay distance. This set of graphs for H_f = 20 feet and the indicated cases (after Bretschneider).

that for fixed decay distances and fetch periods T_F, the shorter the fetch the greater the period increase. Furthermore, for the same fetch period, the shorter the fetch the

swifter the fall-off of the relative height H_D/H_F with D. To see this intuitively, note that larger wind speeds are needed to generate a given wave period in shorter fetches; the resultant waves are higher and steeper and consequently decay more quickly (the nonlinear wave-dissipating mechanisms are more effective in waves of *finite* amplitude).

A complementary situation to that in Fig. 12.39(a) is depicted in Fig. 12.39(b) in which the common datum is now an H_F of 20 feet.

The general shape of the curves is such that, on theoretical grounds, the energy content of the waves should ultimately decrease exponentially, a fact which holds for both large and small fetches and hydrosol depths. However, initial rates of decay are governed by the geometry of the initial waves, and their initial fetch, and are generally not of a simple exponential type. (In analogy to the asymptotic radiance theorem of Chapter 10, there may be a precisely phrasable and valid counterpart in ocean wave propagation theory, so that in the limit, ocean waves decay at a rate independent of their origin and dependent only on the inherent hydrodynamic and geometric structure of the hydrosol.)

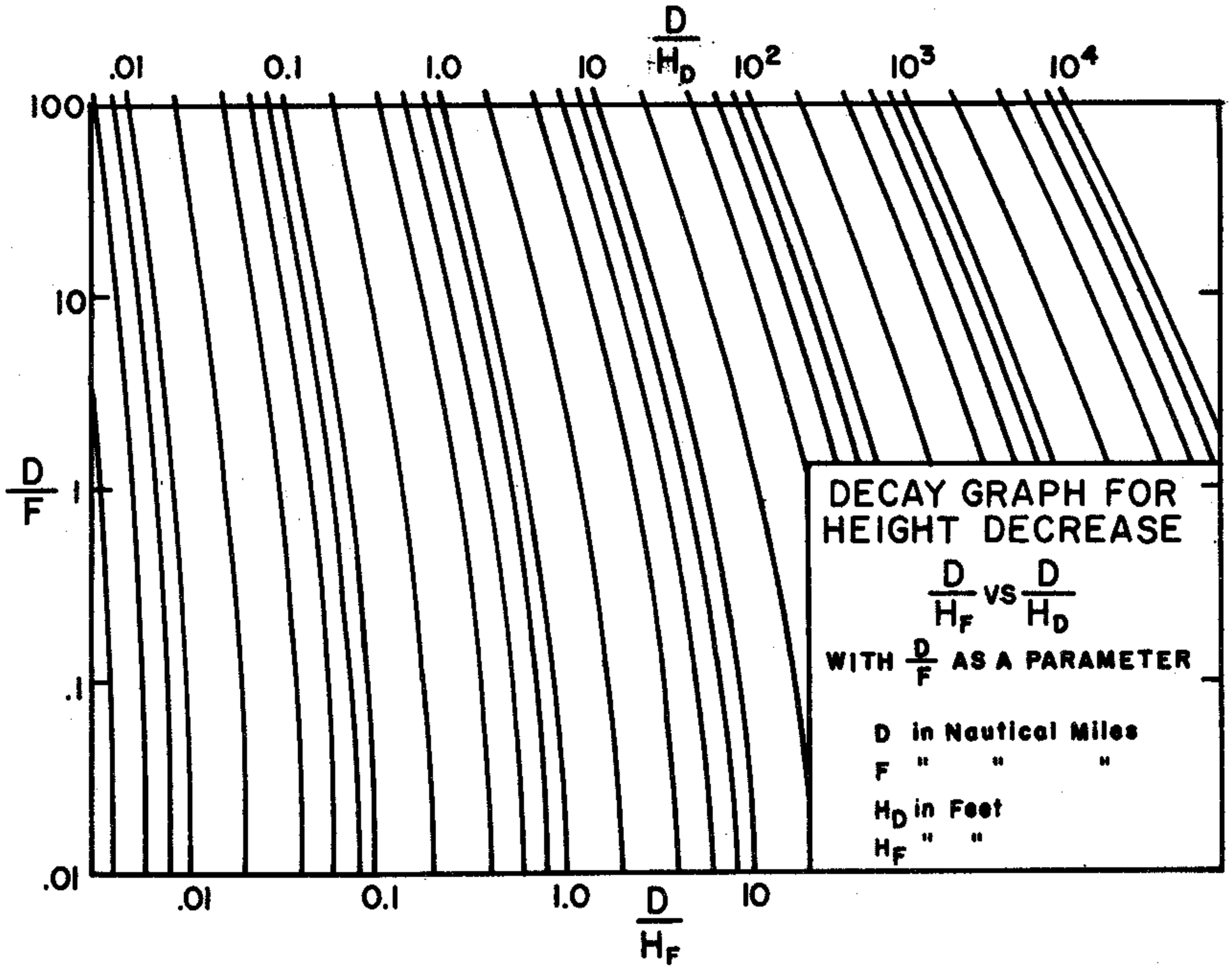

FIG. 12.40(a) Relationships between fetch, wave period at end of fetch, decay, and wave period at end of decay (after Bretschneider).

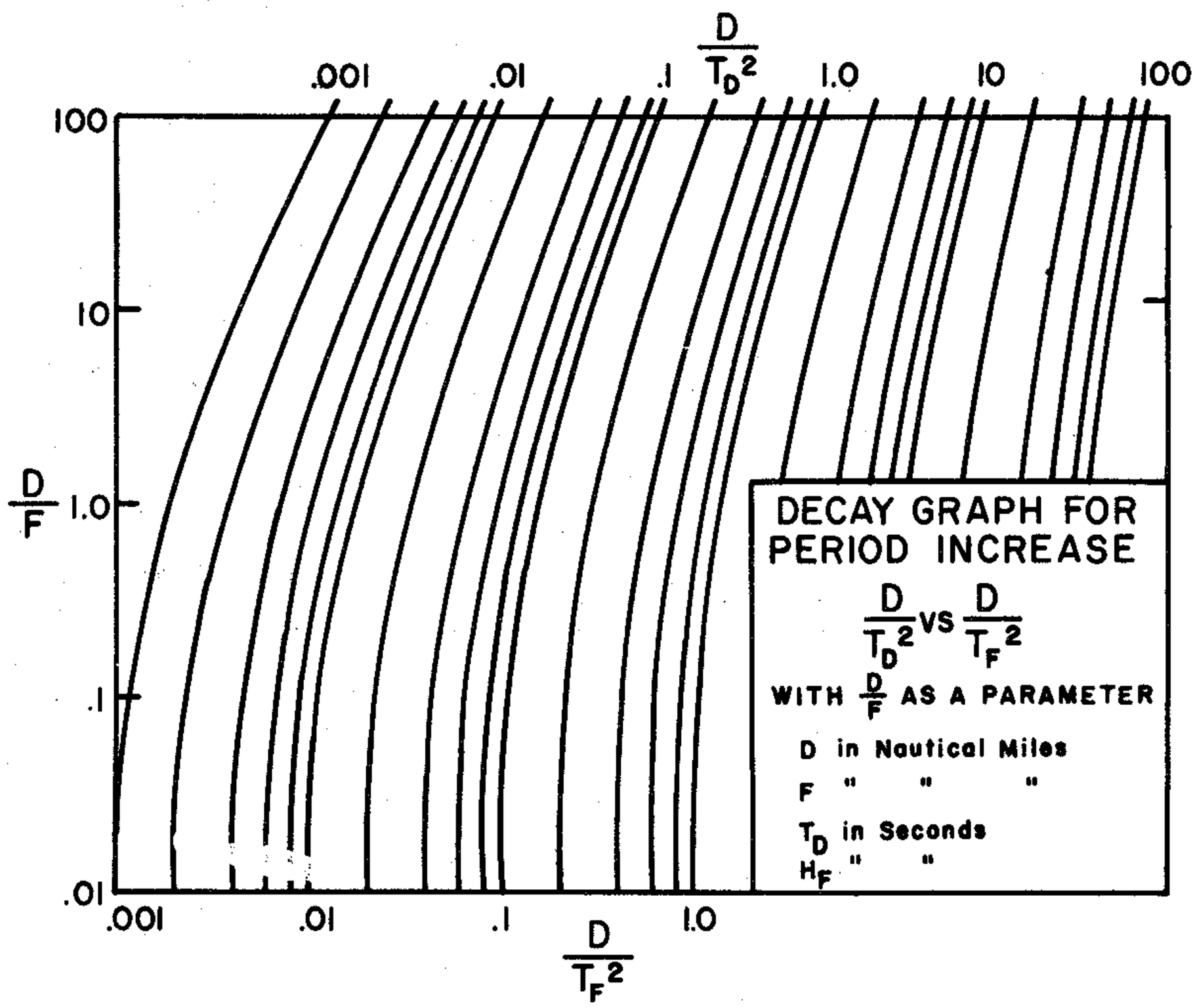

FIG. 12.40(b) Relationships between fetch, wave height at end of fetch, decay, and wave period at end of decay (after Bretschneider).

Figures 12.40(a) and 12.40(b) depict the general empirical relations governing the decay of waves, as compiled by Bretschneider [32]. Figure 12.40(a) depicts D/H_F vs. D/H_D with D/F as parameter. Hence this figure may be used to find H_D knowing the fetch F, decay distance D and H_F. Figure 12.40(b) on the other hand may be used to find T_D given T_F and D, exactly analogously to the example given above for H. For example, to find H_D when H_F = 5 feet, F = 20 nautical miles, and D = 20 nautical miles; form the ratios D/F = 1, D/H_F = 4. Starting at ordinate D/F = 1 on the left hand scale of Fig. 12.40(a), move to the right until the abscissa D/H = 4 is reached. This point lies between the D/H_D curve 6 and the D/H_D curve 8. Let us say that it lies on the D/H_D curve 7. Then

$$\frac{D}{H_D} = 7$$

so that

$$H_D = D/7 = 20/7 = 2.85 \text{ feet} \quad .$$

<< Table of Contents << Title Page >> Next Page >>